Traffic 2008; **9:** 1925–1935
Blackwell Munksgaard

doi: 10.1111/j.1600-0854.2008.00802.x

HIV-1 Nef Induces a Rab11-Dependent Routing of Endocytosed Immune Costimulatory Proteins CD80 and CD86 to the Golgi

Ashutosh Chaudhry[1], Suman Ranjan Das[2], Shahid Jameel[2], Anna George[1], Vineeta Bal[1], Satyajit Mayor[3,*], and Satyajit Rath[1,*]

[1]National Institute of Immunology, Aruna Asaf Ali Road, New Delhi 110067, India
[2]International Centre for Genetic Engineering and Biotechnology, Aruna Asaf Ali Road, New Delhi 110067, India
[3]National Centre for Biological Sciences, GKVK Campus, Bellary Road, Bangalore 560065, India
**Corresponding author: Satyajit Mayor, mayor@ncbs.res.in and Satyajit Rath, satyajit@nii.res.in*

The Nef protein of HIV-1 removes the immune costimulatory proteins CD80 and CD86 from the cell surface by a unique clathrin- and dynamin-independent, actin-based endocytic pathway that deploys coupled activation of *c-src* and Rac. In this study, we show that, similar to major histocompatibility complex class I (MHCI), Nef subsequently reroutes CD80 and CD86 to the Golgi region. However, not only are CD80/CD86 internalized by a different mechanism from MHCI but also the vesicular pathway of Golgi delivery for CD80/CD86 is distinct from that employed for MHCI. While MHCI passes through early endosomal and sorting compartments marked by Rab5/early embryonic antigen 1 and ADP ribosylation factor 6, respectively, CD80 and CD86 enter endocytic vesicles that do not acquire conventional early endosomal markers but remain accessible to fluid probes. Rather than being delivered to preexisting Rab11-positive recycling compartments, these vesicles recruit Rab11 *de novo*. Rab11 activity is also necessary for the delivery of CD80/CD86 in these transitional vesicles to the Golgi region. These data reveal an unusual pathway of endocytic vesicular traffic to the Golgi and its recruitment in a viral immune evasion strategy.

Key words: clathrin independent, dynamin independent, endocytosis

Received 18 February 2008, revised and accepted for publication 21 July 2008, uncorrected manuscript published online 7 August 2008, published online 28 August 2008

The pleiotropic Nef protein of HIV-1 contributes significantly to viral pathogenicity (1–3). In addition to functions such as preventing apoptosis of infected cells and inducing bystander T-cell activation (4–7), Nef is also reported to contribute to immune evasion by removing major histocompatibility complex (MHC) class I (MHCI) and MHC class II (MHCII) from the surface of infected macrophages (8).

We have recently reported that in cells of the myeloid lineage, Nef binds to and mediates endocytosis of CD80 and CD86, leading to defective antigen-presenting cell function (8). The Nef-mediated endocytic mechanisms operating on CD80 and CD86 are distinct from those mediating MHCI internalization. First, mutations in Nef preventing MHCI downmodulation do not affect CD80 and CD86 endocytosis (8). Furthermore, Nef-mediated removal of CD80 and CD86 from the cell surface, unlike MHCI removal, is not sensitive to cholesterol depletion or phosphatidylinositol kinase (PIK) inhibition by wortmannin (Wm). Instead, the removal of CD80/CD86 involves a two-pronged strategy involving *c-src* and Rac (9). On the one hand, Nef expression triggers phosphorylation of *c-src*, leading to downstream activation of the small guanosine triphosphatase (GTPase) Rac through a GTP exchange factor called Tiam (9). In another arm of this pathway, Nef specifically binds to the cytosolic tails of CD80 and CD86 to mark them for Rac-mediated endocytosis (9). None of these molecular elements is shared by the mechanism involved in Nef-mediated removal of cell surface MHCI.

Despite this difference in the molecular programs mediating Nef-triggered endocytosis, MHCI and CD80/CD86 appear to be relocated to the same intracellular compartment (8). The relocation of MHCI by Nef is thought to be mediated not by enhanced endocytosis *per se* but by rerouting of MHCI molecules in their constitutive recycling program to deliver them to the Golgi region as the final destination (10–12). This delivery is dependent on ADP ribosylation factor 6 (Arf6), although whether it requires the Arf6 molecule directly or simply occurs in a vesicular compartment marked by Arf6 is not yet clear (13).

In this study, we show that Nef-mediated removal of CD80 and CD86 follows a different endocytic pathway from that taken by MHCI. Unlike MHCI, Nef-marked CD80/CD86 enters distinct vesicular compartments that do not possess conventional early endosomal markers. Furthermore, CD80/CD86-containing vesicles acquire the small GTPase, Rab11, without being associated with the normal recycling compartment. Finally, the CD80/CD86 cargo is eventually

delivered from transitional vesicles to the Golgi region by a Rab11-dependent mechanism.

Results

HIV-1 Nef relocates cell surface MHCI, CD80 and CD86 to the Golgi

We have previously shown that in Nef-expressing human U937 monocytic cells, MHCI, CD80 and CD86 are internalized by a unique dynamin-independent endocytic mechanism (8,9). To identify the intracellular compartment where MHCI, CD80 and CD86 were relocated to in Nef-expressing cells, we transfected U937 cells with an expression vector containing the *nef* gene from an HIV-1 subtype C clinical isolate (8) fused in-frame to the *EGFP* gene. At 24-h post-transfection, cells were examined by confocal microscopy. Figure 1 shows that Nef–enhanced green fluorescent protein (EGFP) is colocalized with endogenous MHCI, CD80 and CD86 in intracellular organelles marked by Golgi markers, GM130 and caveolin-2, while no colocalization of organelles containing both Nef–EGFP and accompanying MHCI, CD80 or CD86 was observed with endoplasmic reticulum (ERp72), endosomal

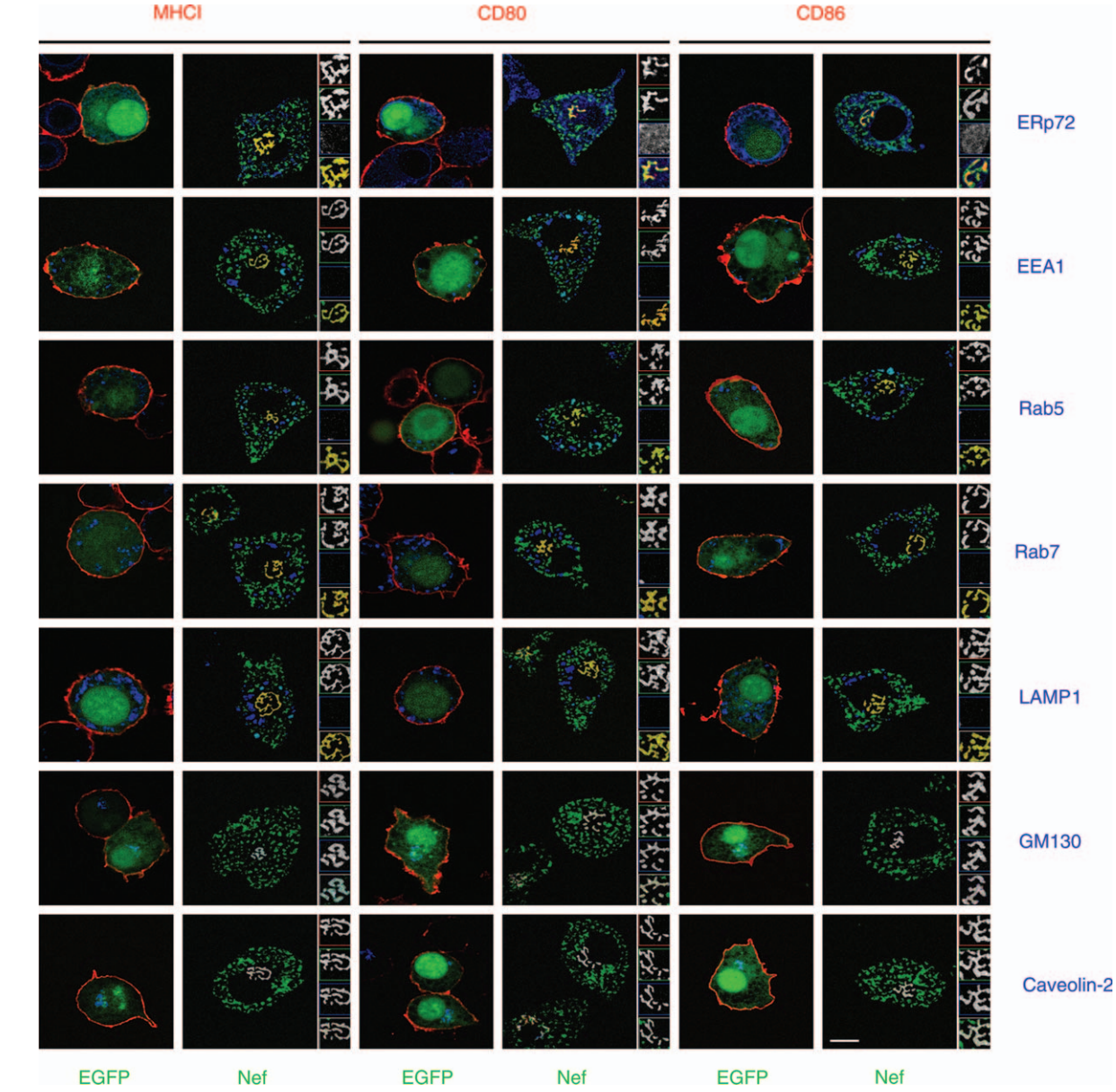

Figure 1: Nef redistributes CD80 and CD86 to the Golgi. U937 cells expressing either control EGFP or Nef–EGFP were fixed and stained for the various molecules shown. Scale bar represents 10 μm. Insets are magnified (×2) and show grayscale images for each color as well as for merged images from the appropriate regions.

[early embryonic antigen 1 (EEA1) and Rab5] or lysosomal markers [Rab7 and lysosome-associated membrane protein-1 (LAMP1)].

We next ascertained that cell surface MHCI, CD80 and CD86 internalized by the activity of Nef were relocated from the cell surface to the Golgi (GM130-marked compartments) by tracking antibody-labeled surface molecules. For this, Nef-transfected U937 cells were labeled with fluorochrome-tagged antibodies against cell surface MHCI, CD80 or CD86 and examined by confocal microscopy. By 12-h post-surface labeling, MHCI, CD80 and CD86 molecules had disappeared from the surface of Nef-expressing cells but not from control EGFP-expressing U937 cells. They were relocated in GM130-bearing compartments along with Nef–EGFP (Figure 2A). As additional confirmation of the intracellular destination of Nef-induced CD80 and CD86, we disrupted the morphology of the Golgi using the fungal toxin, Brefeldin A (14). Colocalization with the Golgi marker, GM130, persisted in cells even where the organization of the Golgi was disrupted by Brefeldin A (Figure S1A). Furthermore, greater than 75% of the internalized fluorescence intensity of MHCI, CD80 and CD86 was colocalized with GM130, 12-h post-internalization (Figure S1B), consistent with the Golgi as the site of intracellular delivery of CD80 and CD86.

Internalization of MHCI exhibited relatively rapid kinetics and could be visualized as early as 1-h post-surface labeling, while downregulation of CD80 and CD86 was relatively slower and was clearly evident only by 4 h (Figure 2B; quantification in Figure S2).

Nef redistributes surface MHCI and CD80/CD86 to the Golgi by distinct pathways

Using the approach outlined above, we examined intermediate stages of internalization of MHCI, CD80 and CD86 in Nef-expressing cells and assessed their colocalization

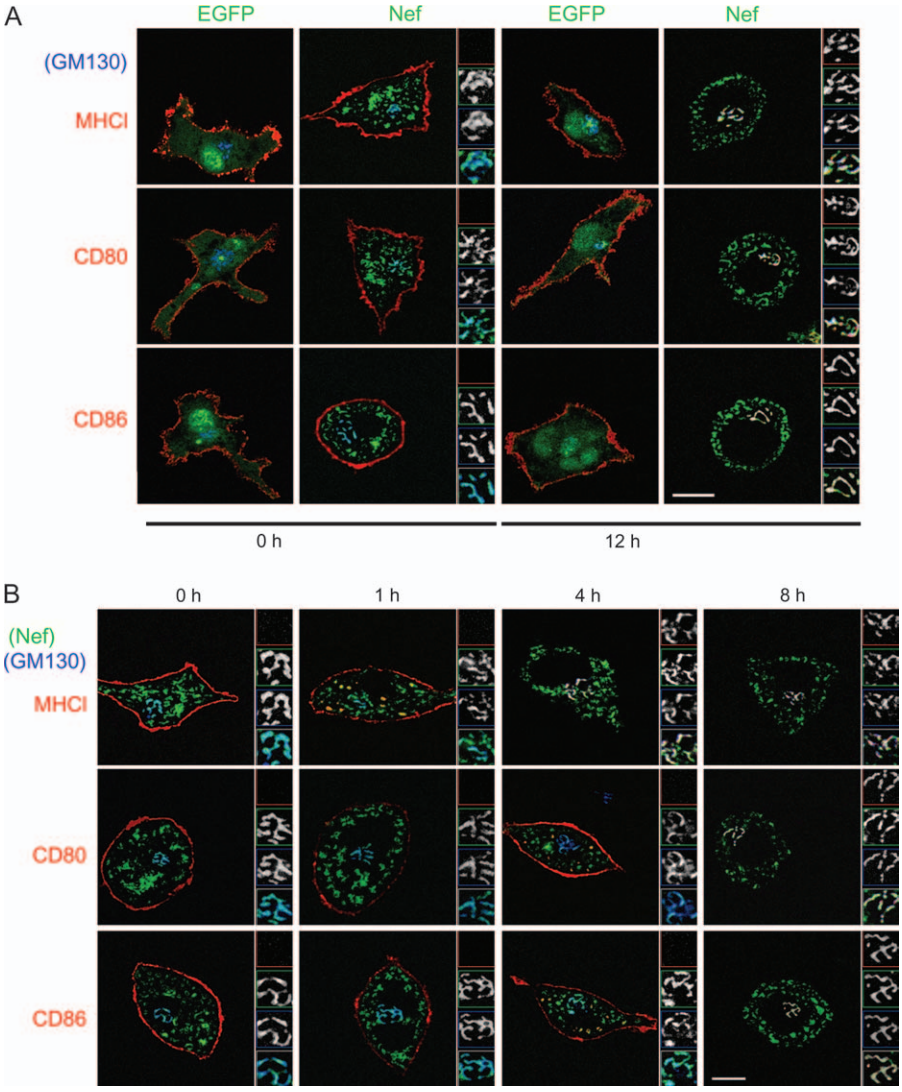

Figure 2: Nef traffics internalized MHCI, CD80 and CD86 to the Golgi. A) U937 cells were transfected to express EGFP or Nef–EGFP, followed, 8 h later, by labeling cell surface MHCI, CD80 or CD86 with biotinylated antibodies on ice. Cells were then shifted to 37°C and cultured further for periods indicated before being fixed and stained for GM130, followed by confocal microscopy. Insets are magnified (×2) and show grayscale images for each color as well as for merged colors. B) U937 cells expressing Nef–EGFP were labeled for cell surface MHCI, CD80 or CD86 as in (A) above and cultured further for indicated times before being fixed and stained for GM130 and imaged by confocal microscopy. Insets are magnified (×2) and show grayscale images for each color as well as for merged colors. Scale bar, 10 μm.

with a range of vesicular and endosomal markers (Figure 3A–G). While internalized vesicles containing MHCI, CD80 or CD86 colocalized with the Nef protein at all times, distinct patterns of transient marker colocalization emerged for MHCI versus CD80 and CD86.

The majority of internalized MHCI molecules in Nef-expressing cells colocalized with vesicles carrying Rab5 and EEA1 (Figure 3A) by 30 min. By the end of 2 h, MHCI-carrying endosomes had lost these markers and showed some degree of colocalization with Arf6 (Figure 3A). No detectable overlap of internalized MHCI vesicles was observed with the late endosomal marker, Rab7, or the recycling endosomal marker, Rab11 (Figure 3B). By 3 h onwards, MHCI-carrying endosomes progressively lost Arf6 and accumulated in Rab6- and GM130-marked compartments (Figure 3C). At early time-points, internalized MHCI molecules also colocalized transiently with a short pulse of endocytosed transferrin (Tf) (Figure 3D), whereas cointernalized fluorescent dextran (Dex), which predominantly marks late endosomes, did not show any significant colocalization (Figure 3D).

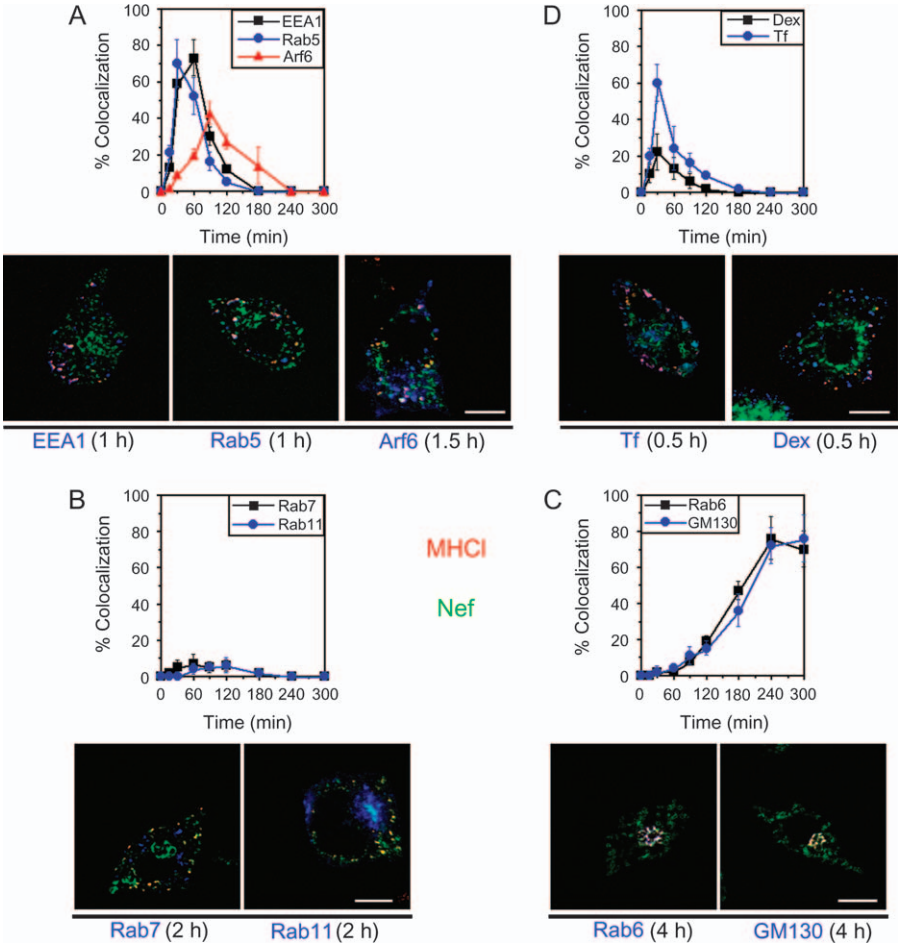

Figure 3: Vesicular pathway for Nef-mediated trafficking of internalized MHCI. A) Transfected U937 cells expressing Nef–EGFP were labeled for MHCI with fluorophore-conjugated antibodies at the cell surface and incubated for various times as indicated. For detection of Arf6, U937 cells were cotransfected with plasmids expressing Nef–HA and Arf6–EGFP. At each time-point shown, surface label was stripped and cells were permeabilized and stained for EEA1 or Rab5. Cells were then imaged by either high-resolution wide-field fluorescence microscopy or confocal microscopy. B) U937 cells coexpressing Nef–HA along with EGFP–Rab11 were labeled for MHCI with fluorophore-conjugated antibodies at the cell surface and incubated for various times as indicated. For detection of Rab7, U937 cells expressing Nef–EGFP were stained for Rab7. At each time-point shown, surface label was stripped and cells were permeabilized and stained for Nef. Cells were then imaged by either high-resolution wide-field fluorescence microscopy or confocal microscopy. C) U937 cells transfected with Nef–EGFP were labeled for MHCI with fluorophore-conjugated antibodies at the cell surface and incubated for various times as indicated. At indicated time-points, surface label was stripped and cells were permeabilized and stained for Rab6 or GM130. Cells were then imaged by either high-resolution wide-field fluorescence microscopy or confocal microscopy. D) Nef-expressing U937 cells were pulsed with fluorophore-labeled Tf or Dex for 10 min, immediately after surface labeling for MHCI. At indicated time-points, surface label was stripped and cells were imaged by either high-resolution wide-field fluorescence microscopy or confocal microscopy. Images of Nef-expressing cells were quantified for the fraction of internalized MHCI colocalizing with the various markers shown. Data are plotted as the extent of colocalization over time (mean ± SE, $n = 100$ cells). Scale bar, 10 μm.

However, surface-labeled CD80 and CD86 molecules followed an altogether different route under the influence of Nef. First, using an acid-strip procedure, which removes >90% of the surface label, neither CD80 nor CD86 was detectably internalized until at least 2-h post-surface labeling (Figure S2). Second, upon internalization, at no time-point did CD80/CD86-bearing vesicles show any detectable colocalization with Rab5, EEA1 or Arf6 (Figure 4A). CD80- and CD86-containing vesicles also did not acquire the late endosomal marker Rab7 (Figure 4B). Instead, by 4 h, these vesicles acquired the small GTPase Rab11 (Figure 4B), a recycling endosome marker (15). Finally, by 6 h, CD80 and CD86 were delivered to Rab6- and GM130-positive Golgi compartments (Figure 4C). When these cells were pulse labeled with endocytosed probes, fluorescent Tf or Dex, at 3 h after surface labeling with anti-CD80/CD86 antibodies, internalized CD80 and CD86 molecules showed no colocalization with Tf, although they were accessible to endocytosed Dex at early time-points (Figure 4D). Together, these results suggest that Nef redirects MHCI from early endosomal compartments to the Golgi consistent with previous studies (13), whereas CD80 and CD86 are internalized to the Golgi by a different endocytic route.

Nef-induced CD80/CD86-containing vesicles recruit cytoplasmic pool of Rab11

To examine the pathway that delivers Nef-marked CD80/CD86 to the Golgi, we focused on the transient colocalization of CD80 and CD86 with Rab11 just prior to delivery to the Golgi. The colocalization with Rab11 could be the result of fusion with *bona fide* Rab11-positive recycling endosomes or by independent recruitment of Rab11 to the transitional vesicles, which are formed by a distinct dynamin-independent pathway (9). To differentiate between these two possibilities, U937 cells were transfected with either a control *ECFP* gene or the *nef* gene fused in-frame to *ECFP* gene and surface labeled with tagged anti-CD80 or anti-CD86 antibodies to track endocytosed CD80/CD86. These cells were then pulsed with labeled Tf to mark the entire recycling pathway and subsequently examined by confocal microscopy (Figure 5A). If the colocalization of Rab11 and CD80/CD86 occurred in Tf-marked recycling endosomes, delivery of CD80/CD86 vesicles to the Golgi must involve fusion with the recycling endosomes. However, a lack of colocalization with the Tf-marked recycling pathway would indicate *de novo* recruitment of Rab11 separately from the recycling compartment. The data were quantified to examine the extent of colocalization (Figure 5B). Vesicles showing colocalization of Rab11 and CD80/CD86 (Figure 5A, cyan vesicles in insets; and Figure 5B) showed practically no overlap with the Tf-marked Rab11-positive recycling endosomal compartments (Figure 5A, yellow vesicles in insets; and Figure 5B). Furthermore, in control cells expressing EGFP, $79 \pm 10\%$ of the Rab11 structures colocalized with endocytosed Tf, whereas in Nef-transfected cells, only $52 \pm 7\%$ was colocalized with Tf. The remaining Rab11 structures that did not contain Tf were associated with Nef and endocytosed CD80 (or CD86)-marked compartments. This indicated that CD80 and CD86 vesicles were not delivered to Rab11-positive recycling endosomal compartments and, instead, acquired Rab11 in an independent recruitment event, prior to accumulation in the GM130-labeled Golgi compartments.

The colocalization of Rab11 with Nef-containing endocytic vesicles suggested an interaction between Nef and Rab11. We examined this possibility by immunoprecipitating Nef from transfected U937 cells and looking for the coprecipitation of Rab11 by western blotting. Rab11 was found to be associated with Nef (Figure 5C), although it is not yet clear if this association is functionally significant for Rab11-mediated delivery of CD80/CD86 cargo to the Golgi.

Delivery of CD80/CD86 cargo from transitional endocytic vesicles to the Golgi is Rab11 dependent

We next determined if Rab11 is required for the delivery of endocytosed CD80 and CD86 to the Golgi compartment. For this, U937 cells were cotransfected to express both Nef–enhanced cyan fluorescent protein (ECFP) and green fluorescent protein-tagged versions of either the wild-type (WT) or a dominant-negative (DN) mutant of Rab11 (Rab11aS25N) (16) (Figure 6A). The data were quantified to examine the extent of colocalization of CD80 and CD86 and Golgi markers (Figure 6B). In cells expressing Nef and WT-Rab11, CD80 and CD86 continued to be delivered to GM130-marked regions (Figure 6A,B). However, expression of DN-Rab11 prevented the delivery of CD80 and CD86 to GM130-bearing compartments (Figure 6A,B), without inhibiting the internalization of cell surface CD80 or CD86. In DN-Rab11-expressing cells, CD80 and CD86 accumulated in vesicular structures distinct from the Golgi (Figure 6A).

To confirm the involvement of Rab11, we used Rab11a- and Rab11b-specific small interfering RNAs (siRNAs) in cotransfection assays with Nef. An equimolar mixture of Rab11a- and Rab11b-specific siRNA reduced the cellular levels of Rab11 but not of related proteins Rab4, Rab5 and Rab7 (Figure 6C). While the silencing of endogenous Rab11 resulted in a redistribution of endocytosed Tf-containing endosomes (data not shown), it consistently abrogated trafficking of internalized CD80/CD86 vesicles to the Golgi (Figure 6D). However, it had no effect on the net amount of Nef-mediated internalization of CD80 and CD86 (Figure 6E). Thus, Rab11 activity is required for the delivery of internalized CD80 and CD86 to the Golgi region but not for internalization. This effect is specific for the processing of CD80 and CD86 by Nef because Rab11 depletion had no effect on the Nef-mediated delivery of MHCI to the Golgi region (Figure S3). Together, these results suggest that Rab11 is specifically recruited to the Nef-marked CD80/CD86 endosomes to deliver them to the Golgi region.

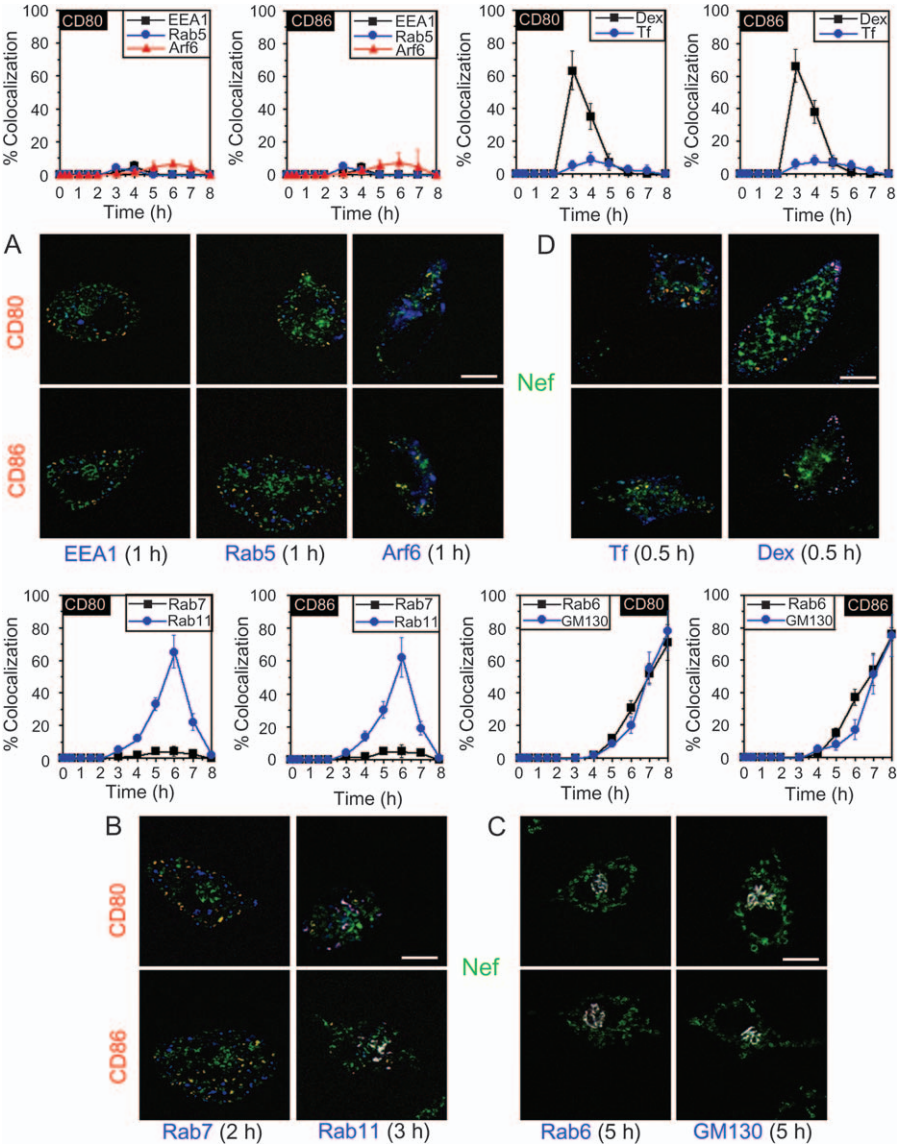

Figure 4: Vesicular pathway for Nef-mediated trafficking of internalized CD80 and CD86. A) Transfected U937 cells expressing Nef–EGFP were labeled for CD80 or CD86 with fluorophore-conjugated antibodies at the cell surface and incubated for various times as indicated. At each time-point shown, surface label was stripped and cells were permeabilized and stained for EEA1 or Rab5. Cells were then imaged by either high-resolution wide-field fluorescence microscopy or confocal microscopy. B) U937 cells coexpressing Nef–HA along with either EGFP–Rab11 or EGFP–Arf6 were labeled for CD80 or CD86 with fluorophore-conjugated antibodies at the cell surface and incubated for various times as indicated. For detection of Arf6, U937 cells were cotransfected with plasmids expressing Nef–HA and Arf6–EGFP. At each time-point shown, surface label was stripped and cells were permeabilized and stained for Nef. Cells were then imaged by either high-resolution wide-field fluorescence microscopy or confocal microscopy. C) U937 cells transfected with Nef–EGFP were labeled for CD80 or CD86 with fluorophore-conjugated antibodies at the cell surface and incubated for various times as indicated. For detection of Rab7, U937 cells expressing Nef–EGFP were stained for Rab7. At indicated time-points, surface label was stripped and cells were permeabilized and stained for Rab6 or GM130. Cells were then imaged by either high-resolution wide-field fluorescence microscopy or confocal microscopy. D) Nef-expressing U937 cells were pulsed with fluorophore-labeled Tf or Dex for 10 min, immediately after surface labeling for CD80 or CD86. At indicated time-points, surface label was stripped and cells were imaged by either high-resolution wide-field fluorescence microscopy or confocal microscopy. Images of Nef-expressing cells were quantified for the fraction of internalized CD80 or CD86 colocalizing with the various markers shown. Data are plotted as the extent of colocalization over time (mean $\pm$ SE, $n = 100$ cells). Scale bar, 10 μm.

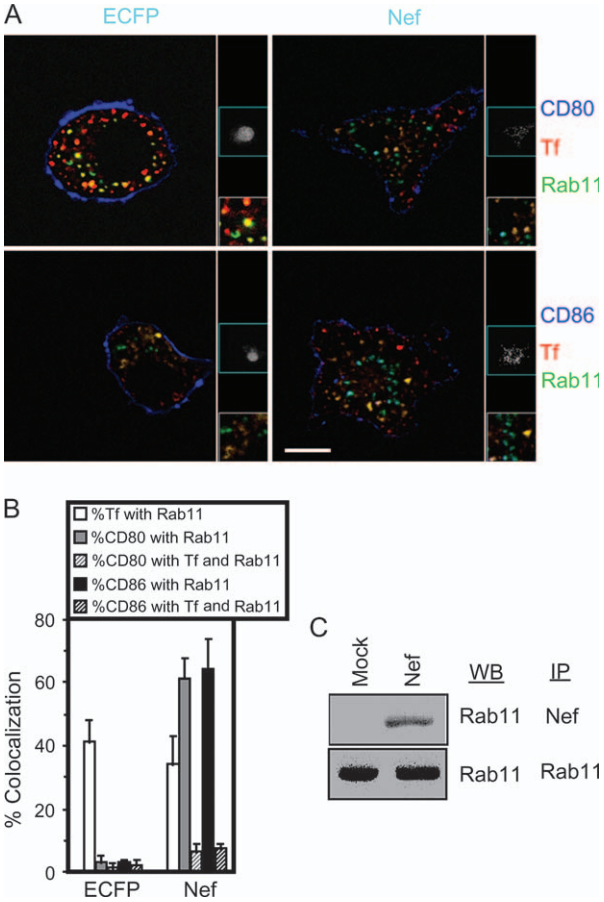

Figure 5: *De novo* recruitment of Rab11 by Nef. A) U937 cells were cotransfected for expression of Nef–ECFP or control ECFP (cyan, grayscale) and EGFP–Rab11 (green). Cells were surface labeled with anti-CD80 or anti-CD86 (blue) antibodies at 8-h post-transfection and incubated for 4 h with fluorophore-labeled Tf. Cells were subsequently imaged by confocal microscopy. Nef or control ECFP is shown as grayscale images. Vesicles showing colocalization (blue vesicles, inset) of Rab11 and CD80 (top half) or CD86 (bottom half) show no overlap with vesicles showing colocalization of Tf and Rab11 (yellow vesicles, inset). Scale bar, 10 μm. B) Images of control ECFP- or Nef–ECFP-expressing cells from above were quantified for the fraction of internalized Tf, CD80 or CD86 colocalizing with various markers as shown (mean ± SE, $n = 50$ cells). C) Lysates from mock-transfected or Nef-transfected U937 cells were immunoprecipitated with anti-Nef antibody and western blotted with anti-Rab11 antibody.

PI3K activity is required for sorting of CD80/CD86 vesicles to the Golgi

PI3K plays an essential role in endocytosis by generating phosphatidylinositol phosphates that in turn serve as docking signals for Rab GTPases on endosomal membranes (15). Inhibition of PI3K has multiple effects, since it is an important regulator of phosphoinositides on the endomembrane system (17). We therefore tested if PI3K was also important in the recycling endosome-independent recruitment of Rab11 to the Nef-induced transitional vesicles containing CD80/CD86. As we have previously reported, the PI3K inhibitor Wm did not inhibit the endocytic removal of CD80 or CD86 from the cell surface (8). However, treatment of U937 cells coexpressing Nef–ECFP and Rab11–EGFP with Wm (100 nM) resulted in sequestration of CD80 and CD86 into vesicles that did not fuse with the Golgi (Figure 7A,B). Furthermore, there was a loss of the normal recruitment of Rab11 to the Nef-induced transitional vesicles carrying CD80/CD86 cargo, accompanied by an altered distribution of Rab11 from a punctate to a diffuse pattern (Figure 7A). As shown previously, Tf delivery to early endosomes (18) and MHCI delivery to the Golgi (13) are also impaired (data not shown).

These data indicate that Nef-mediated delivery of CD80 and CD86 to the Golgi occurs by a *de novo* pathway distinct from the MHCI Golgi relocation pathway and that the transitional vesicles require recruitment of the active GTPase Rab11 as well as PI3K activity to relocate the cargo to the Golgi region.

Discussion

Our results show that in addition to MHCI, Nef mediates the removal of the major cell surface immune costimulatory molecules, CD80 and CD86, to the Golgi region in monocytic cells. Although the relocation of CD80/CD86 superficially resembles MHCI downmodulation in that Nef relocates all three proteins from the cell surface to the Golgi region, the route taken by CD80 and CD86 differs dramatically from that traversed by MHCI. At early time-points during internalization, MHCI as well as CD80 and CD86 are associated with Nef-bearing peripheral endocytic vesicles. However, these vesicles show distinctly different patterns of molecular markers depending on whether they contain MHCI or CD80 and CD86 even if their ultimate target is the Golgi region. Internalized MHCI initially colocalizes with endocytosed Tf and early endosomal markers, EEA1 and Rab5, suggesting that it transits through early endosomes. This is in keeping with the earlier interpretation that this is the normal endocytic pathway of MHCI for constitutive recycling (13). Under normal conditions, MHCI exits these compartments, overlapping with a transient association with Arf6 in recycling endosomes. It is likely that at this point, as previously suggested (13), MHCI is rerouted by Nef to the Golgi.

However, vesicles bearing CD80 and CD86 and internalized in Nef-expressing cells do not colocalize with typical early endosomal markers such as Rab5, EEA1, endocytosed Tf and Arf6 as well as late endosomal markers such as Rab7. Instead, unlike MHCI-containing vesicles, they are accessible to a pulse of endocytosed fluid cargo and acquire the recycling endosomal marker, Rab11. Because CD80- and CD86-containing endocytic vesicles lack the cointernalized recycling marker Tf or the early endosomal marker Rab5, we propose that Rab11 recruitment is *de novo* from the cytoplasm rather than by fusion with recycling endosomes. Furthermore, while the recruitment of Rab11 to Tf-positive recycling endosomes is refractory

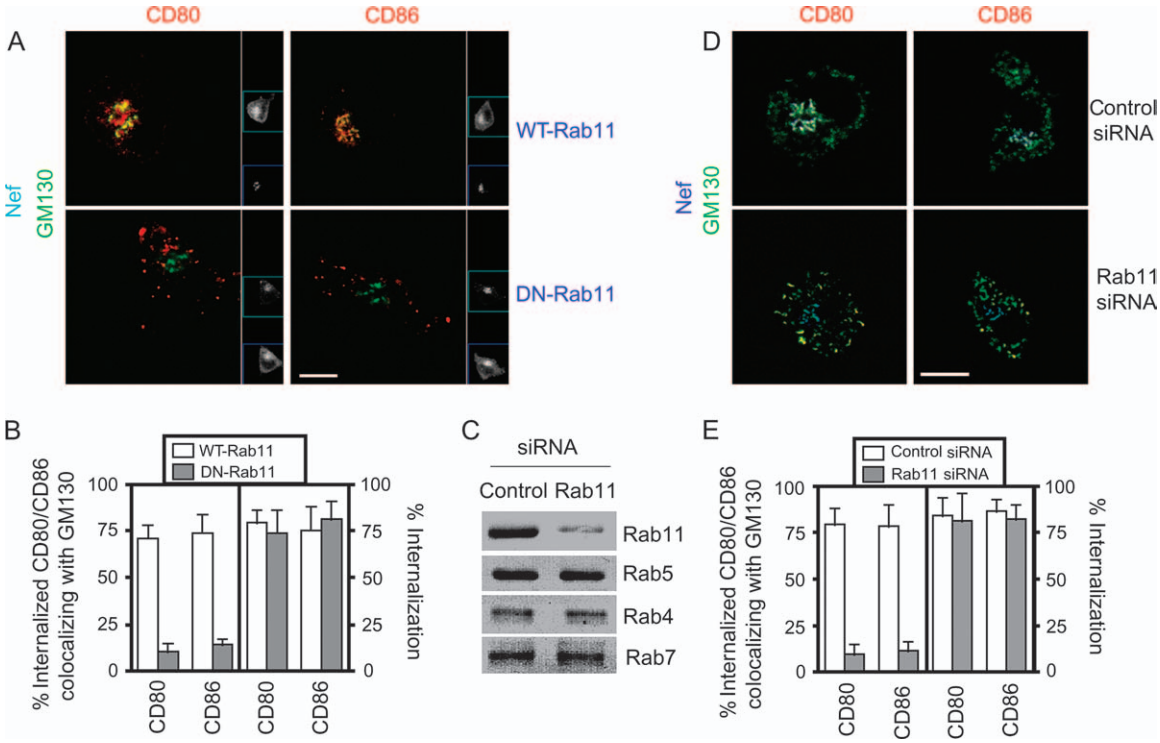

Figure 6: Rab11 recruitment controls sorting of internalized CD80 and CD86 to the Golgi. A) U937 cells were cotransfected for expression of EGFP–Rab11-WT or EGFP–Rab11-DN (blue) as indicated along with Nef–ECFP (cyan). Cells were subsequently stained for CD80 or CD86 (red) as well as GM130 (green) 24 h after transfection and imaged by confocal microscopy. Insets show grayscale images for Nef (cyan) and WT/DN-Rab11 (blue). Note that DN-Rab11 prevents Golgi delivery of internalized CD80 or CD86, which accumulates in large cytoplasmic vesicular structures separate from an intact perinuclear GM130-labeled Golgi. Scale bar, 10 μm. B) Images of Nef-expressing cells from above were quantified for the fraction of total CD80 or CD86 internalized (right panel) and the fraction of internalized CD80 or CD86 colocalizing with GM130 (left panel) (mean ± SE, $n = 50$ cells). C) U937 cells were cotransfected with an equimolar mixture of Rab11a- and Rab11b-specific siRNA or a control siRNA along with a marker Thy-1-expressing plasmid. Magnetic sorting of Thy-1^+ cells was followed by western blot analyses of cell lysates with the indicated antibodies. D) U937 cells were cotransfected for expression of Rab11a siRNA or control siRNA as indicated along with Nef–ECFP. Cells were subsequently stained for CD80 or CD86 (red) as well as GM130 (green) and imaged by confocal microscopy. Insets show grayscale images for Nef in the indicated cells. Scale bar, 10 μm. E) Images of Nef-expressing cells from above were quantified for the fraction of internalized CD80 or CD86 colocalizing with GM130 (mean ± SE, $n = 50$ cells).

to inhibition of PI3K activity (19), Rab11 recruitment to the vesicles carrying CD80 and CD86 is drastically impaired by treatment with Wm. Although, at this stage, a transient 'kiss and run' encounter with a *bona fide* Rab11-bearing recycling compartment cannot be completely ruled out.

Recruitment of Rab11 is necessary for delivery of CD80/CD86 to the Golgi region, because eliminating Rab11 activity inhibits Nef-mediated localization of CD80 and CD86 to Golgi-like regions, but not their internalization. This pathway appears to be a novel mechanism subverted by the virus because conventionally, the role of Rab11 is expected to regulate partitioning of recycling endosome and lysosome-directed cargo selection (20). This subversion may be mediated by the recruitment of Rab11 into a complex nucleated by Nef because we have observed that Nef and Rab11 can be coimmunoprecipitated. Although during the endocytic trafficking of shiga toxin, Rab11 plays a role in efficient *trans* Golgi network (TGN)/Golgi delivery of the toxin from recycling endosomes, in contrast to Nef-mediated CD80/CD86 delivery to the Golgi, expression of WT, DN and dominant-active mutants of Rab11 causes only a small decrease in TGN/Golgi delivery of the toxin (21).

Our data are thus consistent with a trafficking model wherein Nef functions in early endosomes to redirect MHCI to the Golgi, whereas it functions at the cell surface to generate entirely new CD80/CD86-containing vesicles (9), which then recruit Rab11 in a PI3K-dependent fashion to direct them to the Golgi region.

Materials and Methods

Plasmids, cell culture and reagents

The F2-nef gene from an Indian HIV-1 subtype C primary isolate subcloned into the bicistronic mammalian expression vector pIRES2-EGFP (Clontech)

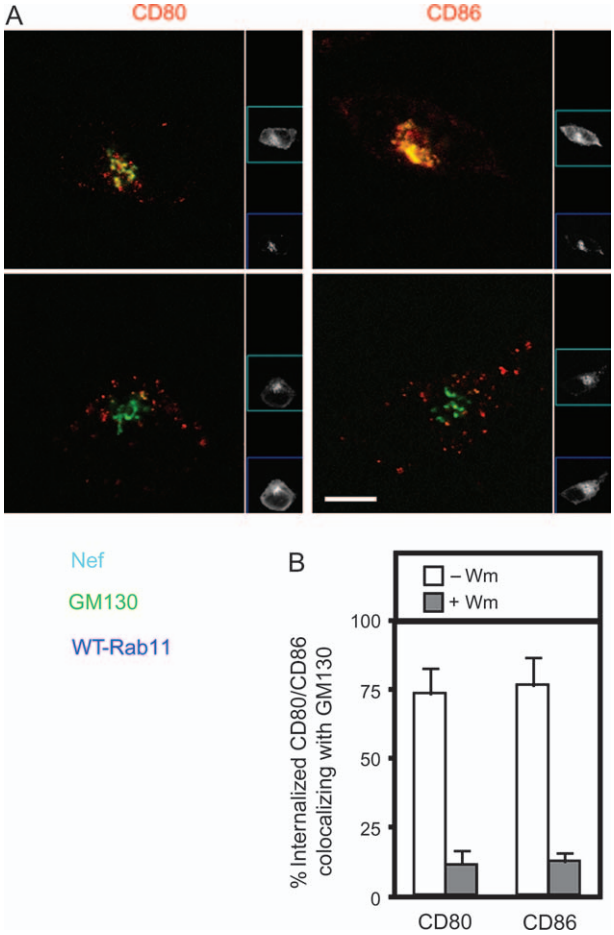

Figure 7: PI3K activity is required for Golgi delivery of internalized CD80 and CD86. A) U937 cells expressing EGFP–Rab 11-WT and F2-Nef–HA were surface labeled with antibodies to CD80 and CD86 at 8-h post-transfection. Cells were then cultured for 4–5 h in presence of Wm (100 nM) and subsequently stained for GM130. Insets show grayscale images for Nef (cyan) and WT-Rab11 (blue). Wm treatment perturbs localization of Rab11 and prevents Golgi delivery of internalized CD80 or CD86. Scale bar, 10 μm. B) Nef-expressing cells were quantified for the fraction of internalized CD80 or CD86 colocalizing with GM130 in the absence or presence of Wm (mean ± SE, $n = 50$ cells).

or expressed as a nef–egfp fusion gene in the plasmid pEGFP-N3 (Clontech) have been described earlier (8). Rab11 and its mutant isoform were the kind gift from Dr Nigel Bunnett (University of California, San Francisco, CA, USA), Arf6–EGFP from Dr Julie Donaldson (National Institutes of Health, Bethesda, MD, USA) and the Thy-1-expressing plasmid from Dr Thomas Mitchell (University of Louisville, Louisville, KY, USA). The Rab11a- and Rab11b-specific siRNAs as well as the control siRNA were commercially obtained (Dharmacon). The nef–ecfp fusion gene was generated by ligating the F2-nef gene into appropriate restriction sites of pECFP-N1 (Clontech).

U937 monocytic cells were maintained in RPMI-1640 medium, with fetal calf serum, antibiotics and lipopolysaccharide (0.5 μg/mL) for maintenance of high MHC, CD80 and CD86 levels. Transfections were done using Fugene6 (Roche), according to the manufacturers' protocols, with 10 μg of plasmid DNA for 1×10^6 cells.

The following reagents were used: fluorophore-labeled Dex [tetramethylrhodamine (TMR)-Dextran; Molecular Probes], Tf (Molecular Probes) and Wm (Sigma). Monoclonal antibodies (mAbs) used were against Rab5, Rab11, EEA1, Rab6, GM130, ERp72, LAMP1 and caveolin-2 (Transduction Laboratories); Rab7 (Santa Cruz Biotech) and p38MAPK (Cell Signaling Technologies). Anti-MHCI (W6/32) was either purified from culture supernatants or used as W6/32–biotin conjugates (Serotec). Purified anti-CD80 and anti-CD86 mAbs (eBiosciences) were labeled by either Cy5 (Amersham) or Alexa dyes (Molecular Probes). Labeled secondary detection reagents used included goat anti-mouse immunoglobulin G (IgG) (Fc)-phycoerythrin (PE), donkey anti-rat IgG (Fc)-PE (Jackson ImmunoResearch), rat anti-mouse Thy-1 (BD PharMingen), streptavidin–Alexa568 and streptavidin–Alexa633 (Molecular Probes). For studies with hemagglutinin peptide (HAp)-tagged molecules, intracellular staining was done using an anti-HA mAb (Cell Signaling Technology).

Cell labeling and other treatments

U937 cells, grown on poly-D-lysine-coated coverslip-bottomed dishes, were transfected with various plasmids and surface labeled 8 h later with either biotinylated or primary labeled anti-MHCI, anti-CD80 or anti-CD86 antibodies on ice for 30 min. Cells were then warmed to 37°C and chased for varying lengths of time.

To visualize the endosomal distribution of the fluorescent tracers, cell surface label (fluorophore-labeled Tf or anti-MHCI, anti-CD80 or anti-CD86) was removed by using a combination of low pH and high pH buffers (ascorbate buffer, pH 4.5, 160 mM sodium ascorbate, 40 mM ascorbic acid, 1 mM $MgCl_2$ and 1 mM $CaCl_2$).

Confocal and wide-field microscopy and image processing

Cells were fixed with 4% paraformaldehyde for 20 min at 37°C and permeabilized using 0.3% Tween-20 or 0.03% saponin in PBS for 20 min at ambient temperature. They were then blocked with 2 mg/mL BSA in PBS prior to incubation with antibodies in the same medium. Rabbit and mouse primary antibodies were detected using fluorophore-labeled Fc-specific anti-rabbit IgG or anti-mouse IgG.

Confocal imaging was performed either on a Bio-Rad MRC 1024 confocal microscope (Bio-Rad Microsciences) or on a Zeiss LSM510 Meta confocal microscope (Zeiss). Confocal imaging on the Bio-Rad MRC 1024 confocal microscope was with factory set dichroics and an argon–krypton laser using the LaserSharp software with a step size of 0.2 μm and a digital zoom of 3.4 corresponding to a pixel size of 0.12 μm. Iris size was kept constant at 3.0 units, and 8-bit images were acquired with a ×60 1.45 numerical aperture (NA) objective. For confocal imaging on a Zeiss LSM510 confocal microscope equipped with argon, HeNe and HeCd lasers, a step size of 0.1 μm and a digital zoom of 3.5 corresponding to a pixel size of 0.10 μm was used. Pinhole size was kept constant at 272 units (optical section <2 μm and Airy units <3), and 12-bit images were collected with a ×63 1.45 NA objective.

High-resolution wide-field images were collected using Nikon TE 300 inverted microscope equipped with ×60 1.4 NA and ×20 0.75 NA objectives, a mercury arc illuminator (Nikon) and a cooled charge-coupled device camera (Princeton Instruments) controlled by Metamorph software (Universal Imaging). Optimized dichroics, excitation and emission filters were used as described (22).

Quantitative colocalization analysis

Colocalization between internalized vesicles and endocytic markers was quantified using two softwares, MultiSpots and MultiColloc (9,23,24), variations of custom-developed software, Spots and Coloc as described previously (23–27). The criteria outlined below were applied to images obtained from U937 cells labeled with antibodies against Rab5, EEA1, Arf6, Rab6, Rab11 and GM130 or pulsed with endocytic tracers Tf and Dex for 10 min at 37°C. High-resolution images of cells labeled with endocytic tracers were obtained using a ×60 1.4 NA objective on a wide-field microscope at a pixel resolution of 0.15 μm/pixel. The images were corrected for background fluorescence using the 'produce background

correction' image procedure in METAMORPH image analysis software using the following parameters suitable for producing a local background image while at the same time preserving the intensity of the endosomes (box size = 30 × 30 pixels, subsample ratio = 10, percentile = 0.2).

The background corrected images were then processed through MULTI-SPOTS to identify endosomes using parameters defined by pixels above a threshold (set by inspection for each image) and area (minimum = 3 pixel, maximum = no upper limit). A trimming procedure was applied to isolate and segregate individual endosomes based on the inclusion of pixels with intensities greater than 0.3 of maximal intensity within a unit of connected pixels having intensity greater than the set threshold. This was achieved by an iterative procedure using a step size (0.01) for each iteration, which limits for the number of iterations of the trimming procedure. The resultant image contains a set of identified 'spots or endosomes' quantified in terms of net intensity per spot and total pixel area per spot.

The two 'spotted' images of different fluorophore-labeled markers were matched up against each other to identify the endosomes wherein the two molecules were colocalized. Endosomes in a tracer image (e.g. CD80-associated endosomes) were compared with endosomes in a reference image (e.g. Rab11-containing endosomes) using MULTICOLOC, and endosomes with 50% or more area overlap were considered to be colocalized. The resultant image displays all the spots that are colocalized using a particular 'tracer-reference' image pair.

Cell outlines were drawn based on the phase contrast image of the cell, and the net intensity of each fluorophore per cell was calculated in the spotted as well as the colocalized images using procedures in METAMORPH. The percentage colocalization was then calculated from the ratio of the net intensity within a cell in the CD80/CD86/MHCI with the appropriate Rab5/EEA1/Rab11/etc endocytic marker MULTICOLOC image to the net spot intensity of the same cell in the MHCI/CD80/CD86 spots image. Maximum extent of colocalization obtained by this method is 90% for the colocalization of cointernalized Alexa568–Tf and Alexa647–Tf in the same cell. Per cent colocalization is represented as a mean and standard error of the mean obtained from three independent experiments with a minimum of 30 cells per data point.

All images were processed for output purposes using ADOBE PHOTOSHOP software (Adobe).

Immunoprecipitation and western blot analyses

Transfected cell lysates were immunoprecipitated with various antibodies as described (9), and western blots for the indicated molecules were performed after 12% SDS–PAGE of 50 μg protein/lane and transfer. The secondary reagents were goat anti-mouse IgG–horseradish peroxidase (HRP) (Cell Signaling Technologies) or donkey anti-rabbit IgG–HRP (Jackson Immunoresearch). Blots were developed with the diaminobenzidine (DAB) reagent (Bio-Rad).

Flow cytometry

Cells were stained with primary and secondary reagents on ice for 30 min, as appropriate. For intracellular staining, cells were permeabilized with 0.3% Tween-20 or 0.03% saponin. Stained cells were analyzed on a BD-LSR flow cytometer (BD Biosciences), and data from ~100 000 cells were routinely acquired for each sample. Data were analyzed using FLOWJO software (Treestar). All data shown are representative of three to five independent experiments.

Acknowledgments

This study was supported in part by grants from the Departments of Science and Technology and Biotechnology, Government of India (A. G., S. R. and V. B.), and the Indian Council of Medical Research (S. R. and V. B.). S. M. gratefully acknowledges a Swarnajayanti fellowship from the Department of Science and Technology, Government of India. We are grateful to Drs Nigel Bunnett (University of California), Julie Donaldson (National Institutes of Health) and Thomas Mitchell (University of Louisville) for generously providing reagents. We acknowledge Dr H. Krishnamurthy (National Centre for Biological Science, Bangalore) for his help with the use of the Imaging Facility at National Centre for Biological Science supported by Welcome Trust Equipment Grant and a grant from the Department of Science and Technology. The National Institute of Immunology and the International Centre for Genetic Engineering and Biotechnology are supported by the Department of Biotechnology, Government of India.

Supporting Information

Additional Supporting Information may be found in the online version of this article:

Figure S1: Nef expression induces delivery of cell surface CD80 and CD86 to GM130-marked compartments. A) Nef-induced internalization of cell-surface-labeled CD80 and CD86 was observed in GFP–Nef-expressing cells, 12 h after surface labeling with specific antibodies. Cells were incubated in the presence of Brefeldin (+BfA) or absence of Brefeldin (−BfA) for the last hour of the chase period. CD80 and CD86 antibodies were stripped from the cell surface, the cells were fixed, then permeabilized and stained for GM130 (blue), and the internalized antibodies (red) were detected, all as described in experimental procedures. Scale bar, 10 μm. B) The extent of colocalization of internalized MHCI, CD80 and CD86 with the indicated compartment markers was determined as detailed in experimental procedures and shown as a fraction of the internalized fluorescence intensity, 12 h after addition of antibodies to the cell surface proteins. Note that MHCI, CD80 and CD86 are all extensively colocalized with markers of the Golgi (GM130 and Cav2) but not with markers of the endoplasmic reticulum (ERp72), the early endosome (EEA and Rab5) or the late endosome (Rab7 and LAMP1).

Figure S2: Time–course for Nef-induced downregulation of MHCI, CD80 and CD86. Cell surface levels of MHCI, CD80 and CD86 were ascertained by quantifying the amount of surface-localized antibodies at the indicated times post-surface labeling ($t = 0$) with protein-specific antibodies directed against MHC1, CD80 and CD86. The level of fluorescence was quantified by flow cytometry, and the mean fluorescence intensity ± SE were obtained from three independent data sets for each time-point. The data shown are representative of at least eight different experiments [see also (1,2)]. Note that MHCI is relatively rapidly internalized at the cell surface compared with CD80 and CD86.

Figure S3: Internalization and destination of MHCI are unaffected in Rab11-siRNA-expressing cells. U937 cells were cotransfected for expression of Rab11a siRNA or control siRNA as indicated along with Nef–ECFP (cyan). Cells were subsequently incubated with antibodies against MHCI (left panels) for 12 h and stained for MHCI (red) as well as for GM130 (green) or incubated with fluorescent Tf (right panels) for 30 min, prior to imaging by confocal microscopy. Insets show grayscale images for Nef (cyan outline) in control/Rab11-shRNA-treated cells. Scale bar, 10 μm. Note that MHCI continues to be delivered to the Golgi, whereas the distribution of internalized Tf in Rab11a-siRNA-treated cells is drastically altered.

Please note: Wiley-Blackwell are not responsible for the content or functionality of any supporting materials supplied by the authors. Any queries (other than missing material) should be directed to the corresponding author for the article.

References

1. Kestler HW III, Ringler DJ, Mori K, Panicali DL, Sehgal PK, Daniel MD, Desrosiers RC. Importance of the nef gene for maintenance of high virus loads and for development of AIDS. Cell 1991;65:651–662.
2. Mariani R, Kirchhoff F, Greenough TC, Sullivan JL, Desrosiers RC, Skowronski J. High frequency of defective nef alleles in a long-term survivor with nonprogressive human immunodeficiency virus type 1 infection. J Virol 1996;70:7752–7764.
3. Greenway AL, Holloway G, McPhee DA, Ellis P, Cornall A, Lidman M. HIV-1 Nef control of cell signalling molecules: multiple strategies to promote virus replication. J Biosci 2003;28:323–335.
4. Swingler S, Mann A, Jacque J, Brichacek B, Sasseville VG, Williams K, Lackner AA, Janoff EN, Wang R, Fisher D, Stevenson M. HIV-1 Nef mediates lymphocyte chemotaxis and activation by infected macrophages. Nat Med 1999;5:997–1103.
5. Swingler S, Brichacek B, Jacque JM, Ulich C, Zhou J, Stevenson M. HIV-1 Nef intersects the macrophage CD40L signalling pathway to promote resting-cell infection. Nature 2003;424:213–219.
6. Wolf D, Witte V, Laffert B, Blume K, Stromer E, Trapp S, d'Aloja P, Schurmann A, Baur AS. HIV-1 Nef associated PAK and PI3-kinases stimulate Akt-independent Bad-phosphorylation to induce anti-apoptotic signals. Nat Med 2001;7:1217–1224.
7. Geleziunas R, Xu W, Takeda K, Ichijo H, Greene WC. HIV-1 Nef inhibits ASK1-dependent death signalling providing a potential mechanism for protecting the infected host cell. Nature 2001;410:834–838.
8. Chaudhry A, Das SR, Hussain A, Mayor S, George A, Bal V, Jameel S, Rath S. The Nef protein of HIV-1 induces loss of cell surface costimulatory molecules CD80 and CD86 in APCs. J Immunol 2005; 175:4566–4574.
9. Chaudhry A, Das SR, Jameel S, George A, Bal V, Mayor S, Rath S. A two-pronged mechanism for HIV-1 Nef-mediated endocytosis of immune costimulatory molecules CD80 and CD86. Cell Host Microbe 2007;1:37–49.
10. Aiken C, Konner J, Landau NR, Lenburg ME, Trono D. Nef induces CD4 endocytosis: requirement for a critical dileucine motif in the membrane-proximal CD4 cytoplasmic domain. Cell 1994;76:853–864.
11. Greenberg ME, Iafrate AJ, Skowronski J. The SH3 domain-binding surface and an acidic motif in HIV-1 Nef regulate trafficking of class I MHC complexes. EMBO J 1998;17:2777–2789.
12. Stumptner-Cuvelette P, Jouve M, Helft J, Dugast M, Glouzman AS, Jooss K, Raposo G, Benaroch P. Human immunodeficiency virus-1 Nef expression induces intracellular accumulation of multivesicular bodies and major histocompatibility complex class II complexes: potential role of phosphatidylinositol 3-kinase. Mol Biol Cell 2003;14:4857–4870.
13. Blagoveshchenskaya AD, Thomas L, Feliciangeli SF, Hung CH, Thomas G. HIV-1 Nef downregulates MHC-I by a PACS-1- and PI3K-regulated ARF6 endocytic pathway. Cell 2002;111:853–866.
14. Doms RW, Russ G, Yewdell JW. Brefeldin A redistributes resident and itinerant Golgi proteins to the endoplasmic reticulum. J Cell Biol 1989; 109:61–72.
15. Ullrich O, Reinsch S, Urbe S, Zerial M, Parton RG. Rab11 regulates recycling through the pericentriolar recycling endosome. J Cell Biol 1996;135:913–924.
16. Roosterman D, Schmidlin F, Bunnett NW. Rab5a and rab11a mediate agonist-induced trafficking of protease-activated receptor 2. Am J Physiol Cell Physiol 2003;284:C1319–C1329.
17. Lindmo K, Stenmark H. Regulation of membrane traffic by phosphoinositide 3-kinases. J Cell Sci 2006;119:605–614.
18. Martys JL, Wjasow C, Gangi DM, Kielian MC, McGraw TE, Backer JM. Wortmannin-sensitive trafficking pathways in Chinese hamster ovary cells. Differential effects on endocytosis and lysosomal sorting. J Biol Chem 1996;271:10953–10962.
19. Hunyady L, Baukal AJ, Gaborik Z, Olivares-Reyes JA, Bor M, Szaszak M, Lodge R, Catt KJ, Balla T. Differential PI 3-kinase dependence of early and late phases of recycling of the internalized AT1 angiotensin receptor. J Cell Biol 2002;157:1211–1222.
20. Moore RH, Millman EE, Alpizar-Foster E, Dai W, Knoll BJ. Rab11 regulates the recycling and lysosome targeting of beta2-adrenergic receptors. J Cell Sci 2004;117:3107–3117.
21. Wilcke M, Johannes L, Galli T, Mayau V, Goud B, Salamero J. Rab11 regulates the compartmentalization of early endosomes required for efficient transport from early endosomes to the trans-Golgi network. J Cell Biol 2000;151:1207–1220.
22. Chatterjee S, Smith ER, Hanada K, Stevens VL, Mayor S. GPI anchoring leads to sphingolipid-dependent retention of endocytosed proteins in the recycling endosomal compartment. EMBO J 2001;20: 1583–1592.
23. Kirkham M, Fujita A, Chadda R, Nixon SJ, Kurzchalia TV, Sharma DK, Pagano RE, Hancock JF, Mayor S, Parton RG. Ultrastructural identification of uncoated caveolin-independent early endocytic vehicles. J Cell Biol 2005;168:465–476.
24. Sabharanjak S, Sharma P, Parton RG, Mayor S. GPI-anchored proteins are delivered to recycling endosomes via a distinct cdc42-regulated, clathrin-independent pinocytic pathway. Dev Cell 2002;2: 411–423.
25. Dunn KW, McGraw TE, Maxfield FR. Iterative fractionation of recycling receptors from lysosomally destined ligands in an early sorting endosome. J Cell Biol 1989;109:3303–3314.
26. Mayor S, Presley JF, Maxfield FR. Sorting of membrane components from endosomes and subsequent recycling to the cell surface occurs by a bulk flow process. J Cell Biol 1993;121:1257–1269.
27. Ghosh RN, Gelman DL, Maxfield FR. Quantification of low density lipoprotein and transferrin endocytic sorting HEp2 cells using confocal microscopy. J Cell Sci 1994;107:2177–2189.